

## Transport properties of suspensions—critical assessment of Beenakker-Mazur method

Karol Makuch and Bogdan Cichocki

Citation: *J. Chem. Phys.* **137**, 184902 (2012); doi: 10.1063/1.4764303

View online: <http://dx.doi.org/10.1063/1.4764303>

View Table of Contents: <http://jcp.aip.org/resource/1/JCPSA6/v137/i18>

Published by the [American Institute of Physics](#).

---

### Additional information on *J. Chem. Phys.*

Journal Homepage: <http://jcp.aip.org/>

Journal Information: [http://jcp.aip.org/about/about\\_the\\_journal](http://jcp.aip.org/about/about_the_journal)

Top downloads: [http://jcp.aip.org/features/most\\_downloaded](http://jcp.aip.org/features/most_downloaded)

Information for Authors: <http://jcp.aip.org/authors>

## ADVERTISEMENT



**ACCELERATE COMPUTATIONAL CHEMISTRY BY 5X.  
TRY IT ON A FREE, REMOTELY-HOSTED CLUSTER.**

[LEARN MORE](#)

# Transport properties of suspensions—critical assessment of Beenakker-Mazur method

Karol Makuch and Bogdan Cichocki

*Institute of Theoretical Physics, Faculty of Physics, University of Warsaw, Hoża 69, 00-681 Warsaw, Poland*

(Received 12 July 2012; accepted 10 October 2012; published online 9 November 2012)

The Beenakker-Mazur method of calculation of transport coefficients for suspensions has been analyzed. The analysis relies on calculation of the hydrodynamic function and the effective viscosity with higher accuracy and comparison of these characteristics to the original Beenakker-Mazur results. Comparison to numerical simulations is also given. Our calculations go along with the idea of Beenakker and Mazur, but avoid unnecessary approximations. Our higher accuracy results differ significantly from results obtained initially by Beenakker and Mazur for volume fractions  $\phi > 25\%$ . Moreover, our results agree with the precise numerical simulations of Abade and Ladd for volume fractions  $\phi < 15\%$  and volume fractions  $\phi \approx 45\%$ , whereas for volume fractions  $15\% < \phi < 40\%$ , we observe pronounced discrepancies. © 2012 American Institute of Physics. [<http://dx.doi.org/10.1063/1.4764303>]

## I. INTRODUCTION

Colloidal suspensions, which are systems consisted of minute particles immersed in liquid, occur widely both in nature and industry. They represent a diverse class of systems. The diversity follows from two factors. First, different kinds of minute particles may be found in a colloidal suspension such as spherical polymers<sup>1</sup> or hard particles. Second, different types of interparticle interactions such as electrostatic, van der Waals,<sup>2</sup> or magnetic interactions<sup>3</sup> can appear. This diversity implies the variety of physical phenomena of practical importance.

Dynamic light scattering is a widespread experimental method used to investigate colloidal suspensions.<sup>4,5</sup> In such experiments, the autocorrelation function of intensity of scattered light is measured. The autocorrelation function contains information about static and dynamical properties of colloidal suspensions. In particular for short-time scales, autocorrelation function is characterized by the hydrodynamic function. Another quantity which also characterizes the short-time behavior of suspensions is low shear, high frequency effective viscosity.<sup>6</sup>

Hitherto, the most comprehensive theory of the above mentioned short-time characteristics is “ $\delta\gamma$  scheme” introduced by Beenakker and Mazur.<sup>7</sup> Originally, it was used for hard-sphere suspensions. Nowadays,  $\delta\gamma$  scheme is applied to charged particles as well.<sup>8–12</sup> This scheme is based on statistical physics considerations. The key point of the theory is to represent macroscopic characteristics of suspensions by series in renormalized fluctuations. In their calculations, Beenakker and Mazur truncated the series to the second order. However, this truncation is not the only approximation assumed in their articles. Due to the technical difficulties, additional approximations were adopted. They rely on the truncation of hydrodynamic matrices by taking into account the lowest order hydrodynamical multipoles only. Consequences of the truncation were not estimated systematically. The aim of the

present work is to study the effect of these additional approximations. To achieve this, we calculate the transport coefficients in frame of the second order  $\delta\gamma$  scheme, but with large number (extrapolated to infinity) of the hydrodynamic multipoles. We compare original Beenakker and Mazur results to the results obtained by us, and to the results of numerical simulations.

The article is organized as follows. In Sec. II, the basic definitions are introduced and expressions for the hydrodynamic function and effective viscosity are given. The Beenakker-Mazur method is formulated in the Sec. III. Section IV is devoted to the presentation and comparison of the results obtained within different approximation schemes. The article is summarized in Sec. V.

## II. MACROSCOPIC CHARACTERISTICS AND GRAND MOBILITY MATRIX

In this article, we focus on colloidal suspension consisted of spherical particles immersed in an incompressible liquid. Brownian dynamics of particles, on proper time scale, can be described by generalized Smoluchowski equation.<sup>13</sup> The equation governs evolution of the probability distribution of particles  $p(\mathbf{R}_1, \dots, \mathbf{R}_N, t)$  in time instant  $t$ , where  $\mathbf{R}_1, \dots, \mathbf{R}_N$  stand for positions of particles. As it turns out, short time behavior of the autocorrelation function of intensity of scattered light at equilibrium is characterized by the hydrodynamic function  $H(q)$ .<sup>5,13</sup> Another quantity characterizing macroscopic behavior of the suspension is high frequency-low shear effective viscosity  $\eta_{\text{eff}}$ .<sup>6</sup>

In order to present the microscopic expressions for hydrodynamic function  $H(q)$  and effective viscosity  $\eta_{\text{eff}}$ , grand mobility matrix should be introduced. This matrix characterizes a response of suspension of freely moving particles in ambient flow under action of forces and torques applied to each particle. The suspension consists of  $N$  identical hard

spherical particles of radius  $a$  immersed in an infinite incompressible Newtonian liquid with shear viscosity  $\eta$ . Inertia of particles and inertia terms in the Navier-Stokes equation are assumed to be negligible. As a consequence, the flow is governed by steady Stokes equations.<sup>14</sup> Mazur and Bedeaux extended steady Stokes equations for the space inside particles in the following way:

$$\nabla p(\mathbf{r}) - \eta \Delta \mathbf{v}(\mathbf{r}) = \mathbf{f}(\mathbf{r}), \quad (1a)$$

$$\nabla \cdot \mathbf{v}(\mathbf{r}) = 0, \quad (1b)$$

introducing induced force densities  $\mathbf{f}(\mathbf{r})$ .<sup>15</sup> Here,  $p(\mathbf{r})$  and  $\mathbf{v}(\mathbf{r})$  stand for pressure and velocity field of the suspension. These equations should be supplemented with appropriate boundary conditions. We consider hard spheres with the stick boundary conditions

$$\mathbf{v}(\mathbf{r}) = \mathbf{U}_i(\mathbf{r}) = \mathbf{V}_i + \boldsymbol{\Omega}_i \times (\mathbf{r} - \mathbf{R}_i) \quad \text{for } |\mathbf{r} - \mathbf{R}_i| \leq a, \quad (2)$$

$$p(\mathbf{r}) = 0 \quad \text{for } |\mathbf{r} - \mathbf{R}_i| \leq a, \quad (3)$$

where  $\mathbf{V}_i$  and  $\boldsymbol{\Omega}_i$  denote translational and rotational velocity of  $i$ th particle.

Due to the above extension, the flow of suspension in all space (i.e., particles and liquid) is given with the aid of Green function<sup>16</sup>

$$\mathbf{v}(\mathbf{r}) = \int d^3 r' \mathbf{G}(\mathbf{r} - \mathbf{r}') \cdot \mathbf{f}(\mathbf{r}'), \quad (4)$$

where Oseen tensor  $\mathbf{G}$ <sup>17</sup> has the following form:

$$\mathbf{G}(\mathbf{r}) = \frac{1}{8\pi\eta} \frac{\mathbf{1} + \hat{\mathbf{r}}\hat{\mathbf{r}}}{|\mathbf{r}|}, \quad \hat{\mathbf{r}} = \frac{\mathbf{r}}{|\mathbf{r}|}. \quad (5)$$

Moreover, the induced force densities  $\mathbf{f}(\mathbf{r})$  are localized only on the surface of particles, that is

$$\mathbf{f}(\mathbf{r}) = \sum_{i=1}^N \mathbf{f}_i(\mathbf{r}) \quad (6)$$

with  $\mathbf{f}_i(\mathbf{r})$  acting on the surface of  $i$ th particle.<sup>18,19</sup>

## A. Friction problem

In order to find the grand mobility matrix, one starts with the friction problem.<sup>20</sup> To do that, let us assume translational velocities  $\mathbf{V}_i$  and rotational velocities  $\boldsymbol{\Omega}_i$  of particles ( $i = 1, \dots, N$ ) immersed in liquid in which initially an ambient flow  $\mathbf{v}_0(\mathbf{r})$  is present. The aim of the friction problem is to calculate the force densities induced on particles,  $\mathbf{f}_i(\mathbf{r})$ .

The solution of Stokes equations (1) for single particle friction problem has the following linear form:

$$\mathbf{f}_1(\mathbf{r}) = \int d^3 r' \mathbf{Z}_0(\mathbf{R}_1, \mathbf{r}, \mathbf{r}') \cdot (\mathbf{U}_1(\mathbf{r}') - \mathbf{v}_0(\mathbf{r}')). \quad (7)$$

Single particle friction operator  $\mathbf{Z}_0$  is localized on the surface of particle.<sup>21</sup> It means that the induced force density  $\mathbf{f}_1(\mathbf{r})$  is localized on the particle surface and its value depends only on the field  $\mathbf{U}_1(\mathbf{r}') - \mathbf{v}_0(\mathbf{r}')$  in points  $|\mathbf{r} - \mathbf{R}_1| = a$ . Equation (7) will have the following form in shorthand notation:

$$\mathbf{f}_1 = \mathbf{Z}_0(1) \cdot (\mathbf{U}_1 - \mathbf{v}_0), \quad (8)$$

where integration symbol and integral variables are omitted, and the position of particle is denoted by its number.

It is worth mentioning that the single particle friction problem has been solved for a variety of boundary conditions, and various kinds of particles, e.g., spherical polymers. Moreover,  $\mathbf{Z}_0$  operator is the only quantity by which boundary conditions enter into the solution of the problem for suspension. In more general case where particles are different than hard spheres, the induced force density  $\mathbf{f}_1$  may be localized not only on the surface, but also inside the particle. In literature, one can find an explicit form of  $\mathbf{Z}_0$  operator for several situations, e.g., those considered in Refs. 22–24.

Due to the linearity of Stokes equations, the solution of the friction problem for single particle given by the Eq. (8) may be used to solve the friction problem for suspension. In this case, the  $i$ th particle in suspension is surrounded by modified ambient flow

$$\mathbf{v}_0(\mathbf{r}) + \sum_{j \neq i} \int d^3 r' \mathbf{G}(\mathbf{r} - \mathbf{r}') \mathbf{f}_j(\mathbf{r}'), \quad (9)$$

which includes ambient flow  $\mathbf{v}_0(\mathbf{r})$ , and also flow induced by the force densities  $\mathbf{f}_j(\mathbf{r})$  acting on every particle except  $i$ . Equation (8), with the above modified ambient flow, leads to the following formula:

$$\mathbf{f}_i = \mathbf{Z}_0(i) \cdot \left( \mathbf{U}_i - \mathbf{v}_0 - \sum_{j \neq i} \mathbf{G} \mathbf{f}_j \right), \quad (10)$$

which is also written in shorthand notation.

The formal solution of the above equation is given by the expression

$$\mathbf{f}_i = \sum_{j=1}^N \mathbf{Z}_{ij}(1 \dots N) (\mathbf{U}_j - \mathbf{v}_0), \quad (11)$$

where friction operator  $\mathbf{Z}_{ij}$  has the following form of scattering series:

$$\begin{aligned} \mathbf{Z}_{ij}(1 \dots N) &= \delta_{ij} \mathbf{Z}_0(i) + (1 - \delta_{ij}) \mathbf{Z}_0(i) \mathbf{G} \mathbf{Z}_0(j) \\ &+ \sum_{k=1}^N \mathbf{Z}_0(i) \mathbf{G} \mathbf{Z}_0(k) \mathbf{G} \mathbf{Z}_0(j) + \dots \end{aligned} \quad (12)$$

The different terms in Eq. (12) correspond to a scattering sequence. The prime symbol indicates summation, where  $k$  is different than neighboring particle indices in scattering sequence.

Equations (11) and (12) represent the formal solution of the friction problem. Those equations can also be used to solve mobility problem. The aim of the mobility problem is to find the response of suspension of freely moving particles in ambient flow  $\mathbf{v}_0(\mathbf{r})$  to external force  $\mathbf{F}_i$  and torque  $\mathbf{T}_i$  acting on them. By the response of the suspension, we mean the velocity of particles (translational  $\mathbf{V}_i$  and rotational  $\boldsymbol{\Omega}_i$ ) and also the force densities  $\mathbf{f}_i(\mathbf{r})$ . Mobility problem may be solved by the partial inversion of the friction problem.<sup>25</sup>

## B. Multipole expansion

The partial inversion mentioned above and other operations on the operators can be carried out with the use of the multipole expansion formalism.<sup>19,26,27</sup> This is a formalism, in which the force densities are represented by their moments

$$\mathbf{f}_i(\mathbf{r}) \rightarrow \begin{bmatrix} \mathbf{F}_i \\ \mathbf{T}_i \\ \mathbf{S}_i \\ \dots \end{bmatrix}. \quad (13)$$

Here, the total force  $\mathbf{F}_i$  and torque  $\mathbf{T}_i$  produced by  $i$ th particle on the fluid, and also  $\mathbf{S}_i$  - symmetric and traceless part of the first moment of the force density are defined as follows:

$$\mathbf{F}_i = \int d^3r \Theta_i(\mathbf{r}) \mathbf{f}_i(\mathbf{r}), \quad (14a)$$

$$\mathbf{T}_i = \int d^3r \Theta_i(\mathbf{r}) (\mathbf{r} - \mathbf{R}_i) \times \mathbf{f}_i(\mathbf{r}), \quad (14b)$$

$$\mathbf{S}_i = \int d^3r \Theta_i(\mathbf{r}) \overline{(\mathbf{r} - \mathbf{R}_i) \mathbf{f}_i(\mathbf{r})}, \quad (14c)$$

where  $\Theta_i(\mathbf{r})$  denotes the characteristic function of  $i$ th particle: it equals 0 whenever  $\mathbf{r}$  points outside the particle, and equals 1 otherwise. Similarly, velocities  $\mathbf{U}_i - \mathbf{v}_0$  have in the multipole expansion formalism the following representation:

$$\mathbf{U}_i(\mathbf{r}') - \mathbf{v}_0(\mathbf{r}') \rightarrow \begin{bmatrix} \mathbf{V}_i - \mathbf{v}_0(\mathbf{R}_i) \\ \boldsymbol{\Omega}_i - \boldsymbol{\omega}(\mathbf{R}_i) \\ \mathbf{g}(\mathbf{R}_i) \\ \dots \end{bmatrix}, \quad (15)$$

where  $\boldsymbol{\omega}(i)$ , and  $\mathbf{g}(i)$  are defined, respectively, in terms of the gradient of ambient flow in the center of a particle

$$\boldsymbol{\omega}(\mathbf{R}) = \frac{1}{2}(\nabla \times \mathbf{v}_0)_{\mathbf{r}=\mathbf{R}}, \quad (16)$$

$$\mathbf{g}(\mathbf{R}) = \frac{1}{2}(\nabla_\alpha \mathbf{v}_{0,\beta} + \nabla_\beta \mathbf{v}_{0,\alpha})_{\mathbf{r}=\mathbf{R}}. \quad (17)$$

Multipole expansion for the force densities, Eq. (13), and for velocities, Eq. (15), determine the multipole expansion of the single particle friction operator  $\mathbf{Z}_0$  and the Green operator  $\mathbf{G}$ . In the multipole picture, they become infinite matrices. The Green operator  $\mathbf{G}(ij)$  depends on the relative position  $\mathbf{R}_i - \mathbf{R}_j$  of the particles  $i,j$ . Their detailed form in the multipole space may be found in Ref. 28.

## C. Mobility problem

With the aid of the multipole expansion, one can partially invert the friction problem obtaining the solution of the mobility problem.<sup>25</sup> The solution has the following linear form:

$$\begin{bmatrix} \mathbf{V}_i - \mathbf{v}_0(\mathbf{R}_i) \\ \boldsymbol{\Omega}_i - \boldsymbol{\omega}(\mathbf{R}_i) \\ -\mathbf{S}_i \\ \dots \end{bmatrix} = \sum_{j=1}^N \begin{bmatrix} \boldsymbol{\mu}_{ij}^{tt} & \boldsymbol{\mu}_{ij}^{tr} & \boldsymbol{\mu}_{ij}^{td} & \dots \\ \boldsymbol{\mu}_{ij}^{rt} & \boldsymbol{\mu}_{ij}^{rr} & \boldsymbol{\mu}_{ij}^{rd} & \dots \\ \boldsymbol{\mu}_{ij}^{dt} & \boldsymbol{\mu}_{ij}^{dr} & \boldsymbol{\mu}_{ij}^{dd} & \dots \\ \dots & \dots & \dots & \dots \end{bmatrix} \begin{bmatrix} \mathbf{F}_j \\ \mathbf{T}_j \\ \mathbf{g}(\mathbf{R}_j) \\ \dots \end{bmatrix}, \quad (18)$$

in which the grand mobility matrix appears. The matrix depends on the position of particles. Its block elements,  $\boldsymbol{\mu}_{ij}^{tt}$ ,  $\boldsymbol{\mu}_{ij}^{tr}$ , etc., are also matrices. The particular blocks are related to a few important problems. For example, velocities  $\mathbf{V}_i$  of freely moving, torque-free particles, on which forces  $\mathbf{F}_j$  act in absence of ambient flow, can be calculated with the use of the  $\boldsymbol{\mu}_{ij}^{tt}$  block. Moreover, the symmetric dipole surface force  $\mathbf{S}_i$ —essential for effective viscosity—of force-free and torque-free particles in shear flow can be calculated by means of the  $\boldsymbol{\mu}_{ij}^{dd}$  block.

The grand mobility matrix, similarly to operator  $\mathbf{Z}_{ij}$  given by Eq. (12), also has the form of scattering sequence.<sup>29</sup> For the sector  $tt$  of the grand mobility matrix from Eq. (18), this fact is expressed by the following formula:

$$\begin{aligned} & \boldsymbol{\mu}_{ij}^{tt}(1 \dots N) \\ &= \mathbf{P}_t \left[ \delta_{ij} \boldsymbol{\mu}_0(i) + (1 - \delta_{ij}) \boldsymbol{\mu}_0(i) \mathbf{P} \mathbf{Z}_0(i) \mathbf{G}(ij) \mathbf{Z}_0(j) \mathbf{P} \boldsymbol{\mu}_0(j) \right. \\ & \quad \left. - \sum_{k=1}^N \boldsymbol{\mu}_0(i) \mathbf{P} \mathbf{Z}_0(i) \mathbf{G}(ik) \hat{\mathbf{Z}}_0(k) \mathbf{G}(kj) \mathbf{Z}_0(j) \mathbf{P} \boldsymbol{\mu}_0(j) \right. \\ & \quad \left. + \dots \right] \mathbf{P}_t. \end{aligned} \quad (19)$$

In the above expression, the single particle mobility matrix  $\boldsymbol{\mu}_0(i)$  is defined as follows:

$$\boldsymbol{\mu}_0(i) = (\mathbf{P} \mathbf{Z}_0(i) \mathbf{P})^{-1}, \quad (20)$$

where operator  $\mathbf{P}$  projects multipole vectors from Eqs. (13) or (15) on the two lowest multipoles and the inversion should be done in space of these two multipoles.  $\mathbf{P}_t$  projects on the first multipole. Single particle convective friction operator<sup>25</sup>  $\hat{\mathbf{Z}}_0$  is defined with the following expression:

$$\hat{\mathbf{Z}}_0(i) = \mathbf{Z}_0(i) - \mathbf{Z}_0(i) \mathbf{P} \boldsymbol{\mu}_0(i) \mathbf{P} \mathbf{Z}_0(i). \quad (21)$$

For the  $dd$  sector of the grand mobility matrix, the scattering series has the following form:

$$\begin{aligned} & \boldsymbol{\mu}_{ij}^{dd}(1 \dots N) = \mathbf{P}_d \left[ \delta_{ij} \hat{\mathbf{Z}}_0(i) - (1 - \delta_{ij}) \hat{\mathbf{Z}}_0(i) \mathbf{G}(ij) \hat{\mathbf{Z}}_0(j) \right. \\ & \quad \left. + \sum_{k=1}^N \hat{\mathbf{Z}}_0(i) \mathbf{G}(ik) \hat{\mathbf{Z}}_0(k) \mathbf{G}(kj) \hat{\mathbf{Z}}_0(j) + \dots \right] \mathbf{P}_d, \end{aligned} \quad (22)$$

where  $\mathbf{P}_d$  is projection on the third multipole of vectors (13) or (15).

## D. Macroscopic characteristics

In the dynamic light scattering experiments, the dynamic structure factor is probed. When the system is at equilibrium, for short-time scales the dynamic structure factor is characterized by the lowest terms of its cumulant expansion. The first cumulant is given by the static structure factor and hydrodynamic function.<sup>5,13</sup> With the aid of the matrix  $\boldsymbol{\mu}_{ij}^{tt}$ , the microscopic expression for the hydrodynamic function can be

introduced along the line of Beenakker and Mazur,

$$H(\mathbf{k}) = \lim_{\infty} \left\langle \frac{1}{N\mu_0} \sum_{i,j=1}^N \hat{\mathbf{k}} \cdot \boldsymbol{\mu}_{ij}^t(\mathbf{R}_1 \dots \mathbf{R}_N) \cdot \hat{\mathbf{k}} \right. \\ \left. \times \exp[i\mathbf{k} \cdot (\mathbf{R}_i - \mathbf{R}_j)] \right\rangle, \quad (23)$$

where  $\mu_0$  stands for the single particle mobility coefficient (defined with formula  $\boldsymbol{\mu}_{i1}^t(\mathbf{R}_1) = \mu_0 \mathbf{1}$  for a single particle, with  $\mathbf{1}$  identity matrix). The brackets represent an equilibrium ensemble average. In addition, the thermodynamic limit  $N \rightarrow \infty$ , with fixed concentration  $n = N/V$ , denoted by  $\lim_{\infty}$ , has been performed. Here,  $V$  is the volume of the system.

Similarly, low shear-high frequency effective viscosity is given by the following expression:

$$\frac{\eta_{\text{eff}}}{\eta} = (1 - A)^{-1}, \quad (24)$$

where

$$A = \frac{1}{10\eta} \lim_{k \rightarrow 0} \lim_{\infty} \left\langle \frac{1}{V} \sum_{i,j=1}^N \exp[-i\mathbf{k}(\mathbf{R}_i - \mathbf{R}_j)] \right. \\ \left. \times [\boldsymbol{\mu}_{ij}^{dd}(1 \dots N)]_{\alpha\beta\beta\alpha} \right\rangle, \quad (25)$$

and the Einstein summation convention for repeating indexes  $\alpha$  and  $\beta$  has been used.

### III. FORMULATION OF $\delta\gamma$ SCHEME

To calculate the hydrodynamic function, one copes with the scattering series given by Eq. (19) whereas in context of the effective viscosity, the scattering series of the form (22) appears. In the former scattering series, there are a few single-particle operators,  $\mu_0$ ,  $\mathbf{Z}_0$ , and  $\hat{\mathbf{Z}}_0$ . In the latter, there is only one,  $\hat{\mathbf{Z}}_0$ . Due to this, the formulation of the Beenakker-Mazur method in their articles differs in details for the effective viscosity and the hydrodynamic function.<sup>7,30,31</sup> In this article, we formulate the Beennakker-Mazur method for the scattering series of the following form:

$$\mathbf{T}_{ij}(1 \dots N) = \delta_{ij} \mathbf{M}(i) + (1 - \delta_{ij}) \mathbf{M}(i) \mathbf{G}(ij) \mathbf{M}(j) \\ + \sum_{k=1}^N \mathbf{M}(i) \mathbf{G}(ik) \mathbf{M}(k) \mathbf{G}(kj) \mathbf{M}(j) + \dots, \quad (26)$$

which for  $\mathbf{M} = -\hat{\mathbf{Z}}_0$  converts to the scattering series given in Eq. (22). In context of the hydrodynamic function, formulation of the Beenakker-Mazur method requires either simple modification of the scheme presented below, or to express both scattering series in the form of Eq. (26). The latter may be found in Ref. 32.

In order to formulate  $\delta\gamma$  scheme for the scattering series given by the expression (26), we follow the idea of Beenakker

and Mazur. To this end, we consider kernel  $\mathcal{T}$ ,

$$\mathcal{T}(\mathbf{R}, \mathbf{R}'; 1 \dots N) = \sum_{i,j=1}^N \delta(\mathbf{R} - i) \mathbf{T}_{ij}(1 \dots N) \delta(\mathbf{R}' - j), \quad (27)$$

which corresponds to the scattering series  $\mathbf{T}$  given with Eq. (26). The kernel  $\mathcal{T}$  is represented in the following form:

$$\mathcal{T} = \mathcal{M} + \mathcal{M} \tilde{\mathcal{G}} \mathcal{M} + \mathcal{M} \tilde{\mathcal{G}} \mathcal{M} \tilde{\mathcal{G}} \mathcal{M} + \dots, \quad (28)$$

where  $\mathcal{M}$  and  $\tilde{\mathcal{G}}$  are integral operators in the multipole space.  $\mathcal{M}$  is defined with expression

$$\mathcal{M}(\mathbf{R}, \mathbf{R}'; 1 \dots N) = \delta(\mathbf{R} - \mathbf{R}') \sum_{i=1}^N \mathbf{M}(\mathbf{R}_i) \delta(\mathbf{R} - \mathbf{R}_i), \quad (29)$$

whereas  $\tilde{\mathcal{G}}$ , which corresponds to  $\mathbf{G}$  operator, with expression

$$\tilde{\mathcal{G}}(\mathbf{R}_i, \mathbf{R}_j) = \begin{cases} \mathbf{G}(\mathbf{R}_i, \mathbf{R}_j) & \text{for } \mathbf{R}_i \neq \mathbf{R}_j \\ 0 & \text{for } \mathbf{R}_i = \mathbf{R}_j \end{cases}. \quad (30)$$

By product of the operators, e.g.,  $\mathcal{M} \tilde{\mathcal{G}}$ , we will mean the following integral:

$$[\mathcal{M} \tilde{\mathcal{G}}](\mathbf{R}, \mathbf{R}'; 1 \dots N) \\ \equiv \int d\mathbf{R}'' \mathcal{M}(\mathbf{R}, \mathbf{R}''; 1 \dots N) \tilde{\mathcal{G}}(\mathbf{R}'', \mathbf{R}'). \quad (31)$$

Note that in Eq. (26) sum over  $i = k$  or  $k = j$  in the scattering sequences is avoided. In the scattering sequence, the operator  $\mathbf{G}(\mathbf{R}_i, \mathbf{R}_j)$  never connects the same particle, i.e.,  $i$  is never equal to  $j$ . This is the reason for using in Eq. (28)  $\tilde{\mathcal{G}}(\mathbf{R}_i, \mathbf{R}_j)$  operator instead of  $\mathbf{G}(\mathbf{R}_i, \mathbf{R}_j)$ . The only difference between  $\mathbf{G}(\mathbf{R}_i, \mathbf{R}_j)$  and  $\tilde{\mathcal{G}}(\mathbf{R}_i, \mathbf{R}_j)$  operators is for  $\mathbf{R}_i = \mathbf{R}_j$ . This trick introduced by Beenakker and Mazur results in the fact that no condition on summation over the particles appears in the scattering series (28).

A key step leading to the formulation of  $\delta\gamma$  scheme is to renormalize  $\tilde{\mathcal{G}}$  and  $\mathcal{M}$  operators appearing in the scattering series (28). This procedure consists in the resummation of so called “ring-selfcorrelations.” “Ring-selfcorrelations” are scattering structures of the following form:

$$\mathbf{M}_R(\mathbf{R}) = \mathbf{M}(\mathbf{R}) [1 - \mathbf{G}_{\langle \mathcal{M}_R \rangle}(\mathbf{R}, \mathbf{R}) \mathbf{M}(\mathbf{R})]^{-1}. \quad (32)$$

The renormalized propagator  $\mathbf{G}_{\langle \mathcal{M}_R \rangle}$  is defined with the equation

$$\mathbf{G}_{\langle \mathcal{M}_R \rangle} = \tilde{\mathcal{G}} (1 - \langle \mathcal{M}_R \rangle \tilde{\mathcal{G}})^{-1}, \quad (33)$$

where the average of the following single-particle operator appears:

$$\mathcal{M}_R(\mathbf{R}, \mathbf{R}'; 1 \dots N) = \delta(\mathbf{R} - \mathbf{R}') \mathbf{M}_R(\mathbf{R}) \sum_{i=1}^N \delta(\mathbf{R} - \mathbf{R}_i). \quad (34)$$

For given one-particle density defined as  $n(\mathbf{R}) = \langle \sum_{i=1}^N \delta(\mathbf{R} - \mathbf{R}_i) \rangle$ , the last three equations determine  $\mathbf{M}_R$ ,  $\mathcal{M}_R$ , and  $\mathbf{G}_{\langle \mathcal{M}_R \rangle}$ .

The resummation of the “ring-selfcorrelations” will be omitted since it requires simple algebraic operations. As it was shown in the original papers of Beenakker and

Mazur,<sup>7,30,31</sup> the operator  $\mathcal{T}$  can be expressed in terms of fluctuations  $\mathcal{M}_R - \langle \mathcal{M}_R \rangle$  by

$$\mathcal{T} = \mathcal{M} + \mathcal{M} \mathcal{G}_{\langle \mathcal{M}_R \rangle} [1 - (\mathcal{M}_R - \langle \mathcal{M}_R \rangle) \tilde{\mathcal{G}}_{\langle \mathcal{M}_R \rangle}]^{-1} \mathcal{M}_R. \quad (35)$$

The  $\tilde{\mathcal{G}}_{\langle \mathcal{M}_R \rangle}$  operator appearing in the above relation is defined with the formula

$$\tilde{\mathcal{G}}_{\langle \mathcal{M}_R \rangle}(\mathbf{R}, \mathbf{R}') = \begin{cases} \mathcal{G}_{\langle \mathcal{M}_R \rangle}(\mathbf{R}, \mathbf{R}') & \text{for } \mathbf{R} \neq \mathbf{R}' \\ 0 & \text{for } \mathbf{R} = \mathbf{R}', \end{cases} \quad (36)$$

and, similarly to the propagator  $\tilde{\mathcal{G}}$  from definition (30), it eliminates connections to the same particle in the scattering series given by Eq. (35). In the  $\delta\gamma$  theory, the renormalized expression, e.g., Eq. (35), is expanded in powers of the fluctuations  $\mathcal{M}_R - \langle \mathcal{M}_R \rangle$  up to certain order and then the average in Eqs. (23) and (25) is performed. This closes the theory.

In the original papers,<sup>7,30,31</sup> Beenakker and Mazur limited themselves to the second order in renormalized fluctuations. In this case, the concentration of particles and two-particle correlation function only are required to perform the average. Moreover, they have taken in their scheme approximate form of Eq. (32)

$$\mathbf{M}_R(\mathbf{R}) = \mathbf{M}(\mathbf{R}) [1 - \mathcal{G}_{\langle \mathcal{M}_R \rangle}(\mathbf{R}, \mathbf{R})|_{\text{diagonal}} \mathbf{M}(\mathbf{R})]^{-1}. \quad (37)$$

Above, the symbol “diagonal” means taking the diagonal part of matrix  $\mathcal{G}_{\langle \mathcal{M}_R \rangle}(\mathbf{R}, \mathbf{R})$ . This diagonality has to be understood in the frame of the basis used in the original papers of Beenakker and Mazur. As authors of  $\delta\gamma$  theory suggest, there should not be significant difference between both formulations.<sup>31</sup> However, definition (32) is natural, whereas definition (37) is not. Indeed, taking diagonal terms depends on basis in which matrices are presented.

In addition, they employed another approximations related to hydrodynamic matrices appearing in calculations. These matrices with  $\mathcal{G}_{\langle \mathcal{M}_R \rangle}$  operator among them are of infinite dimension. The authors truncated them by regarding the lowest order hydrodynamic multipoles only. It is worth noting that they gave an inadequate estimate of the resultant error.

In the present article, we investigate the influence of these hydrodynamical matrix truncations on the original Beenakker-Mazur theory. Namely, we use Eq. (32) instead (37) and use an accurate description of hydrodynamics by taking into account large number of hydrodynamic multipoles (extrapolated to infinity). Details of the latter topic are presented in the Appendix.

#### IV. RESULTS AND DISCUSSION

In the series of articles, Beenakker and Mazur calculated a few macroscopic characteristics of suspensions with the hydrodynamic function  $H(q)$  and high frequency effective viscosity coefficient  $\eta_{\text{eff}}$  among them.<sup>7,30,31</sup> Below, the results calculated within the original Beenakker and Mazur scheme will be denoted by  $\delta\gamma$  (BM) symbol.

We compare their results with our calculations within the same  $\delta\gamma$  theory but with an accurate description of hydrodynamics and without unnecessary approximation given by Eq. (37). For them, the symbol  $\delta\gamma$  will be used. The outcome

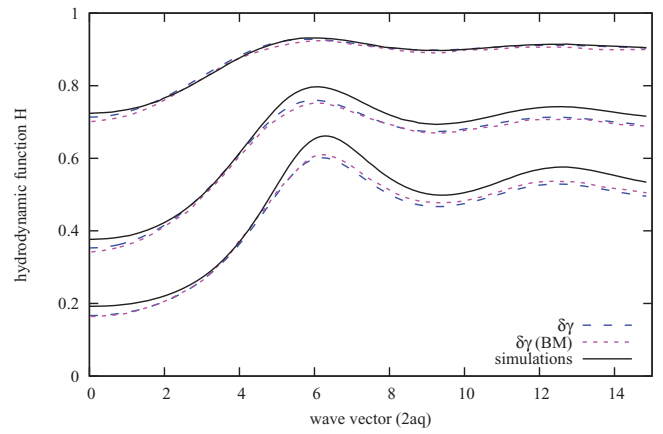


FIG. 1. Hydrodynamic function  $H(q)$  for volume fractions 5%, 15%, and 25% (from top to bottom) in the frame of  $\delta\gamma$  theory at the second order ( $\delta\gamma$ ). Comparison to Beenakker and Mazur results ( $\delta\gamma$  (BM))<sup>31</sup> and numerical simulations of Abade *et al.*<sup>33</sup>

corresponding to the experiments and to the numerical simulations of Abade *et al.*<sup>33</sup> and Ladd<sup>34</sup> are also given.

The hydrodynamic function is presented for volume fraction 5%, 15%, 25% in Figure 1, and for volume fractions 35% and 45% in Figure 2.

The hydrodynamic function from the above figures for zero wave number  $H(0) = K$  (sedimentation coefficient) and for infinite wave-number  $H(\infty) = D_s^s/D_0$  (reduced short time self-diffusion coefficient) are given in Table I. Inverse of those coefficients is also given in Figs. 3 and 4. It should be mentioned that curves are constructed basing on spline interpolation between points following from the tables and from obvious values of transport coefficients for zero volume fraction. In case of reduced low shear, high frequency effective viscosity  $\eta_{\text{eff}}/\eta$  for volume fractions 5%, 15%, 25%, 35%, and 45%, three methods mentioned above give results placed in Table II. The reduced effective viscosity  $\eta_{\text{eff}}/\eta$  is also presented in Fig. 5.

According to the results presented above, differences between the calculations of Beenakker and Mazur and the

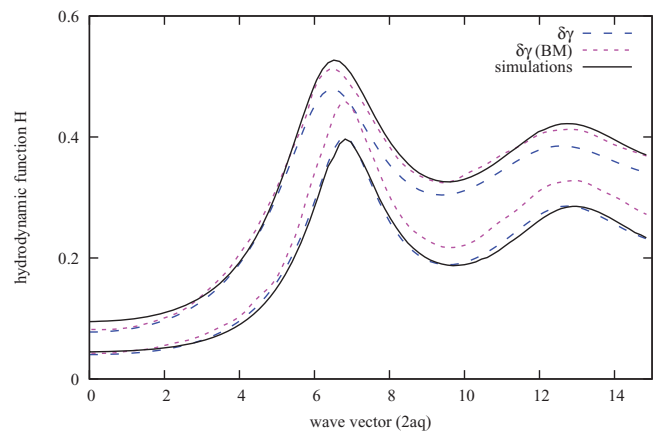


FIG. 2. Hydrodynamic function  $H(q)$  for volume fractions 35% (upper) and 45% (lower) in the frame of  $\delta\gamma$  theory at the second order ( $\delta\gamma$ ). Comparison to Beenakker and Mazur results ( $\delta\gamma$  (BM))<sup>31</sup> and numerical simulations of Abade *et al.*<sup>33</sup>

TABLE I. Reduced selfdiffusion and sedimentation coefficient.

$\phi$ [%]	Reduced self-diffusion $D_s^s/D_0$			Sedimentation $K$		
	$\delta\gamma$	$\delta\gamma$ (BM)	Simulations	$\delta\gamma$	$\delta\gamma$ (BM)	Simulations
5	0.907	0.90	0.908	0.713	0.701	0.724
15	0.699	0.69	0.724	0.353	0.342	0.377
25	0.506	0.51	0.546	0.167	0.164	0.192
35	0.364	0.38	0.383	0.078	0.082	0.0949
45	0.245	0.28	0.243	0.040	0.043	0.0448

calculations of the authors of the present article are not significant up to volume fractions 25%. The discrepancy becomes visible for higher volume fractions. Relative error (with respect to our results) for volume fraction  $\phi = 45\%$  equals 8% in case of sedimentation coefficient, and about 14% for relative self-diffusion and effective viscosity coefficients.

Having compared the results from the original articles by Beenakker and Mazur to the results presented in this article, next we compare our results to numerical simulations. All macroscopic characteristics of suspensions given in the tables above and in corresponding figures have the following tendency. The effective viscosity and the inverse of sedimentation and self-diffusion coefficients are overestimated by the  $\delta\gamma$  theory in almost the whole range of the volume fractions under considerations,  $0 < \phi < 45\%$ . There is a consistency of the results of the  $\delta\gamma$  theory and numerical simulations for volume fraction  $\phi < 15\%$ . Then visible discrepancies appears. The highest relative error (with respect to numerical simulations) is for  $\phi \approx 35\%$ . It equals up to 18% in case of the sedimentation coefficient (this value may be deduced from Table I). For higher volume fractions  $\phi > 35\%$ , the discrepancies decrease and the curves corresponding to the  $\delta\gamma$  theory and numerical simulations tend to intersect. The intersection is evident for the effective viscosity and self-diffusion coefficient.

The discrepancy for volume fractions  $\phi > 25\%$  between the original Beenakker-Mazur calculations and the calculations presented in this paper is caused by the approximations

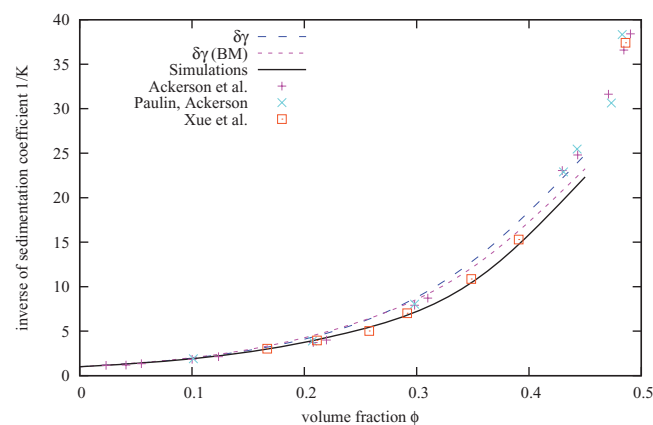


FIG. 3. Inverse of sedimentation coefficient  $1/K$  as a function of volume fraction  $\phi$  in the frame of  $\delta\gamma$  theory at the second order ( $\delta\gamma$ ). Comparison to Beenakker and Mazur results ( $\delta\gamma$  (BM)),<sup>31</sup> numerical simulations of Abade *et al.*,<sup>33</sup> and experiments.<sup>35–37</sup>

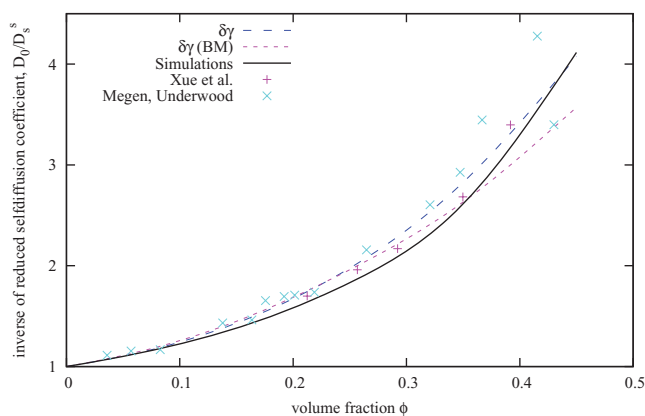


FIG. 4. Inverse of reduced selfdiffusion coefficient  $D_0/D_s^s$  as a function of volume fraction  $\phi$  in frame of  $\delta\gamma$  theory at the second order ( $\delta\gamma$ ). Comparison to Beenakker and Mazur results ( $\delta\gamma$  (BM)),<sup>31</sup> numerical simulations of Abade *et al.*,<sup>33</sup> and experiments.<sup>37,38</sup>

of Beenakker and Mazur. The approximations give reasonable outcome for the volume fractions less than 25%. For higher volume fractions, more comprehensive hydrodynamic description has to be taken.

To shed light on our results obtained in frame of the  $\delta\gamma$  theory in comparison to numerical simulations, we invoke the following fact. In the physics of suspensions, three features of hydrodynamic interactions are often exhibited: their long range, many body character, and strong hydrodynamic interactions of close particles (lubrication corrections). The  $\delta\gamma$  theory at the second order takes account of the first two factors, but not the third one. It properly treats long range hydrodynamic interactions and their many-body character is grasped even in the lowest order by renormalization of the particle response, i.e., resummation of “ring-selfcorrelations.” The third factor is omitted. In fact, to fully take into account strong interactions of close particles, that is in order to fully take into account two body hydrodynamic interactions, one has to go beyond the  $\delta\gamma$  theory with finite order in renormalized fluctuations. Lack of lubrication corrections is the main reason for the discrepancies in the range of the volume fractions  $\phi > 15\%$ . The effective viscosity is overestimated and the sedimentation and self-diffusion coefficients are underestimated in this regime up to the intersection points.

Lubrication corrections are also indispensable to describe properly the transport coefficients for the highest volume fractions, where the effective viscosity tends to infinity and the sedimentation and self-diffusion coefficients vanish, as the experiment shows. Rough treatment of lubrication

TABLE II. Reduced effective viscosity.

$\phi$ [%]	Reduced effective viscosity $\eta_{\text{eff}}/\eta$		
	$\delta\gamma$	$\delta\gamma$ (BM)	Simulations <sup>34</sup>
5	1.15	1.15	1.139
15	1.59	1.59	1.527
25	2.36	2.27	2.17
35	3.67	3.33	3.33
45	5.81	5.00	5.65

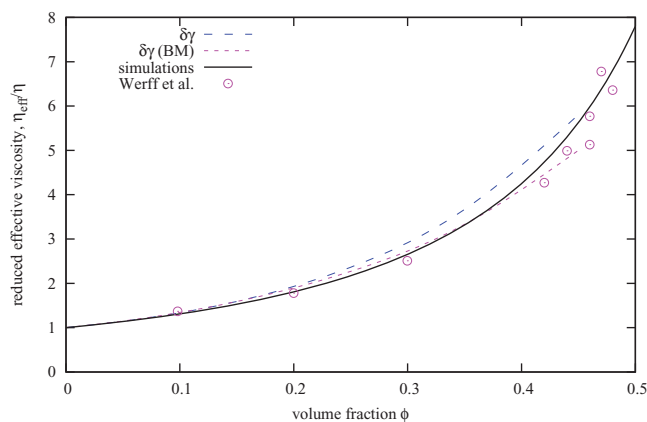


FIG. 5. Reduced high frequency, low shear effective viscosity  $\eta_{\text{eff}}/\eta$  as a function of volume fraction  $\phi$  in the frame of  $\delta\gamma$  theory at the second order ( $\delta\gamma$ ). Comparison to Beenakker and Mazur results ( $\delta\gamma$  (BM)),<sup>30</sup> numerical simulations<sup>34</sup> and experiments.<sup>39</sup>

corrections may thus explain the slope of the curves corresponding to our results in frame of the  $\delta\gamma$  theory. They show strongly increasing underestimation of the effective viscosity and the inverse of sedimentation and self-diffusion coefficients for very high volume fractions above intersection points, outside the range of calculations presented here.

Lack of lubrication corrections suggests that reasonable agreement of the  $\delta\gamma$  theory outcome with numerical simulations may be accidental in character. In this view, it would be desired to apply the theory to different particles than hard-spheres and ask about the volume fraction for the intersection points described above.

Nevertheless, the overestimation of the proper characteristics for low and intermediate volume fractions and intersection (for  $\phi \approx 45\%$  in case of the effective viscosity and self-diffusion coefficients) and further underestimation for the volume fractions above the intersection points make the theory one of the most successful approaches to describe the short-time behavior of suspensions. This is not at all accidental. Despite of the lack of lubrication in the theory, it has a feature, which remarkably distinguishes it from, e.g., virial expansion. The essence of the  $\delta\gamma$  theory—the resummation of ring-selfcorrelations given in Eq. (35)—includes renormalized operators  $\tilde{\mathbf{G}}_{(\mathcal{M}_R)}$  and  $\mathcal{M}_R$ . These operators depend on infinite number of particles, and in consequence, even in the lowest order the  $\delta\gamma$  theory contains the collective behavior of particles in suspension and treats long-range hydrodynamic interactions properly.

## V. SUMMARY

In the present article, macroscopic characteristics of suspensions such as hydrodynamic function and low shear, high frequency effective viscosity have been calculated in the frame of the  $\delta\gamma$  theory at the second order. Although Beenakker and Mazur carried out similar calculations about thirty years ago, they adopted additional approximations, which have been avoided in our work.

Despite our more accurate calculations give larger discrepancies from numerical simulations than the original

Beenakker and Mazur results for intermediate volume fractions, the  $\delta\gamma$  theory is still the most comprehensive statistical physics theory for the description of short-time behavior of suspensions. It takes into account long-range hydrodynamic interactions and their many-body character. The lubrication corrections are omitted in the theory, which limits its applicability for not too high volume fractions. For this reason, the theory able to incorporate the lubrication corrections would be desired.

It is also worth noting that higher accuracy  $\delta\gamma$  scheme presented in this article may be simply adopted to suspensions consisted of different spherical particles than hard spheres (e.g., spherical drops, spherical polymers). The scheme may also be simply adopted to different distributions of particles through the change of two-body correlation function.

## ACKNOWLEDGMENTS

The authors would like to thank Gustavo Abade for the numerical values of the hydrodynamic function obtained in the numerical simulations and Marco Heinen for the results of Beenakker and Mazur calculations of transport coefficients. We are grateful to Piotr Szymczak for reading the manuscript and for his comment. We thank Katarzyna Makuch, Banhi Chatterjee, Joanna Szykuła, and Nevill Gonzalez Szwacki for editorial suggestions. K.M. also acknowledges the support by the Foundation for Polish Science (FNP) through the TEAM/2010-6/2 project co-financed by the EU European Regional Development Fund. The early stage of this work was co-financed by the European Social Fund and the Polish National Budget in frame of the Integrated Regional Development Programme, Action 2.6 - Regional Innovation Strategy and Knowledge Transfer of the Masovian Voivodship project “Mazovian Doctoral Scholarship.”

## APPENDIX: DETAILS OF CALCULATIONS

The calculation of macroscopic characteristics of suspensions in frame of the  $\delta\gamma$  theory requires to solve Eqs. (32)–(34) first, and then to use the solution in expressions for transport coefficients given by Eqs. (23) and (24). These expressions for macroscopic characteristics have been taken at the second order along the line of Beenakker and Mazur. At this order, the volume fraction and two-particle correlation function are required as an input to the equations. As Beenakker and Mazur, we have used the Percus-Yevick approximation for the latter.

To solve the equations of the  $\delta\gamma$  theory, we have represented them in the complex multipole basis.<sup>19,26,27</sup> In this basis, the appropriate operators, e.g.,  $\mathcal{M}_R$  and  $\tilde{\mathbf{G}}$ , become the infinite matrices indexed by three set of numbers:  $l = 1, 2, \dots, \infty$  and  $m = -l, \dots, l$ , and  $\sigma = 0, 1, 2$ . In our calculations, the matrices have been truncated by taking into account multipoles with  $l \leq L$ . We have performed a series of numerical calculations with  $L = 4, \dots, 12$ . Due to strong dependence on truncation  $L$ , the results for the transport coefficients have been extrapolated with  $L \rightarrow \infty$ .

Below, we explain the extrapolation procedure for the effective viscosity. For the volume fraction  $\phi = 45\%$ , its

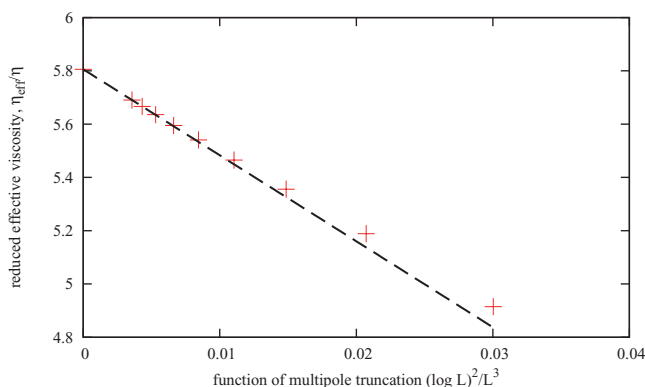


FIG. 6. Reduced high frequency, low shear effective viscosity  $\eta_{\text{eff}}/\eta$  for volume fraction 45% as a function of  $(\log L)^2/L^3$ , where  $L$  stands for the truncation parameter for hydrodynamic multipoles (see text).

dependence on the following function on truncation parameter  $f(L) = (\log L)^2/L^3$  is presented in Fig. 6. The extrapolated effective viscosity is determined as the intersection point of the line passing through points corresponding to  $L = 11$  and  $L = 12$  with vertical axis in Fig. 6. The values of effective viscosity from Table II are obtained with this extrapolation procedure. It should be emphasized that the only motivation for the *ad hoc* choice of  $f$  function is to make the curves for big  $L$  close to straight line. Unfortunately, the authors do not know any theoretical predictions of these asymptotes. For the hydrodynamic function, the extrapolation procedure is similar— with the same function  $f(L)$ .

<sup>1</sup> *Microgel Suspensions: Fundamentals and Applications*, edited by A. Fernandez-Nieves, H. Wyss, J. Mattsson, and D. Weitz (Wiley VCH, 2011).

<sup>2</sup> W. Russel, D. Saville, and W. Schowalter, *Colloidal Dispersions* (Cambridge University Press, 1992).

<sup>3</sup> S. Odenbach, *Colloidal Magnetic Fluids: Basics, Development and Application of Ferrofluids* (Springer, 2009), Vol. 763.

<sup>4</sup> B. Berne and R. Pecora, *Dynamic Light Scattering: With Applications to Chemistry, Biology, and Physics* (Dover, 2000).

<sup>5</sup> G. Nägele, *The Physics of Colloidal Soft Matter* (Centre of Excellence for Advanced Materials and Structures, 2004).

<sup>6</sup> C. G. de Kruif, A. Woutersen, and J. Mellema, *J. Chem. Phys.* **97**, 3857 (1992).

<sup>7</sup> C. W. J. Beenakker and P. Mazur, *Phys. Lett. A* **98**, 22 (1983).

<sup>8</sup> U. Genz and R. Klein, *Physica A* **171**, 26 (1991).

<sup>9</sup> G. Nägele, *Phys. Rep.* **272**, 215 (1996).

<sup>10</sup> L. Rojas, R. Vavrin, C. Urban, J. Kohlbrecher, A. Stradner, F. Scheffold, and P. Schurtenberger, *Faraday Discuss.* **123**, 385 (2003).

<sup>11</sup> A. Banchio and G. Nägele, *J. Chem. Phys.* **128**, 104903 (2008).

<sup>12</sup> M. Heinen, A. Banchio, and G. Nägele, *J. Chem. Phys.* **135**, 154504 (2011).

<sup>13</sup> P. Pusey, *Liquids, Freezing and the Glass Transition* (North-Holland, Amsterdam, 1991), pp. 763–942.

<sup>14</sup> S. Kim and S. Karrila, *Microhydrodynamics: Principles and Selected Applications* (Butterworth-Heinemann, Boston, 1991).

<sup>15</sup> P. Mazur and D. Bedeaux, *Physica* **76**, 235 (1974).

<sup>16</sup> O. A. Ladyzhenskaya, *The Mathematical Theory of Viscous Incompressible Flow* (Gordon and Breach, 1963).

<sup>17</sup> C. Pozrikidis, *Boundary Integral and Singularity Methods for Linearized Viscous Flow* (Cambridge University Press, 1992).

<sup>18</sup> P. Mazur and W. Van Saarloos, *Physica A* **115**, 21 (1982).

<sup>19</sup> M. L. Ekiel-Jezewska and E. Wajnryb, “Precise multipole method for calculating hydrodynamic interactions between spherical particles in the Stokes flow,” in *Theoretical Methods for Micro Scale Viscous Flows*, edited by F. Feuillebois and A. Sellier (Transworld Research Network, Kerala, 2009).

<sup>20</sup> R. Schmitz and B. Felderhof, *Physica A* **113**, 103 (1982).

<sup>21</sup> R. Schmitz and B. Felderhof, *Physica A* **113**, 90 (1982).

<sup>22</sup> J. Bławdziewicz, E. Wajnryb, and M. Loewenberg, *J. Fluid Mech.* **395**, 29 (1999).

<sup>23</sup> B. Cichocki, B. Felderhof, and R. Schmitz, *PCH, PhysicoChem. Hydrodyn.* **10**, 383 (1988).

<sup>24</sup> B. Cichocki and B. Felderhof, *J. Chem. Phys.* **130**, 164712 (2009).

<sup>25</sup> B. Felderhof, *Physica A* **151**, 1 (1988).

<sup>26</sup> B. Cichocki, B. Felderhof, K. Hinsén, E. Wajnryb, and J. Bławdziewicz, *J. Chem. Phys.* **100**, 3780 (1994).

<sup>27</sup> B. Cichocki, R. Jones, R. Kutteh, and E. Wajnryb, *J. Chem. Phys.* **112**, 2548 (2000).

<sup>28</sup> B. Cichocki, M. Ekiel-Jezewska, P. Szymczak, and E. Wajnryb, *J. Chem. Phys.* **117**, 1231 (2002).

<sup>29</sup> P. Szymczak and B. Cichocki, *J. Stat. Mech.: Theory Exp.* **2008**, P01025 (2008).

<sup>30</sup> C. W. J. Beenakker, *Physica A* **128**, 48 (1984).

<sup>31</sup> C. W. J. Beenakker and P. Mazur, *Physica A* **126**, 349 (1984).

<sup>32</sup> K. Makuch, “Scattering series in mobility problem for suspensions,” preprint [arXiv:1208.4255](https://arxiv.org/abs/1208.4255) (2012).

<sup>33</sup> G. Abade, B. Cichocki, M. Ekiel-Jezewska, G. Nägele, and E. Wajnryb, *J. Chem. Phys.* **132**, 014503 (2010).

<sup>34</sup> A. J. C. Ladd, *J. Chem. Phys.* **93**, 3484 (1990).

<sup>35</sup> B. Ackerson, S. Paulin, B. Johnson, W. van Megen, and S. Underwood, *Phys. Rev. E* **59**, 6903 (1999).

<sup>36</sup> S. E. Paulin and B. J. Ackerson, *Phys. Rev. Lett.* **64**, 2663 (1990).

<sup>37</sup> J. Xue, E. Herbolzheimer, M. Rutgers, W. Russel, and P. Chaikin, *Phys. Rev. Lett.* **69**, 1715 (1992).

<sup>38</sup> W. Van Megen and S. M. Underwood, *J. Chem. Phys.* **91**, 552 (1989).

<sup>39</sup> J. Van der Werff, C. De Kruif, C. Blom, and J. Mellema, *Phys. Rev. A* **39**, 795 (1989).